Generating Arm-Swing Trajectories in Real-Time Using a Data-Driven Model for Gait Rehabilitation With Self-Selected Speed

Babak Hejrati, *Member, IEEE*, Andrew S. Merryweather, and Jake J. Abbott, *Member, IEEE*

***Abstract*— Gait rehabilitation is often focused on the legs and overlooks the role of the upper limbs. However, a variety of studies have demonstrated the importance of proper arm swing both during healthy walking and during rehabilitation. In this paper, we describe a method for generating proper arm-swing trajectories in real time using only measurements of the angular velocity of a person's thighs, to be used during gait rehabilitation with self-selected walking speed. A data-driven linear time-invariant transfer function is developed, using frequency-response methods, which captures the frequency-dependent magnitude and phase relationship between the thighs' angular velocities and the arm angles (measured at the shoulder, in the sagittal plane), using a data set of 30 healthy adult subjects. We show that the proposed method generates smooth trajectories for both healthy individuals and patients with mild to moderate Parkinson disease. The proposed method can be used in future robotic devices that integrate arm swing in gait rehabilitation of patients with walking impairments to improve the efficacy of their rehabilitation.**

***Index Terms*— Gait training, self-directed walking, shoulder, thigh, frequency response, Parkinson disease.**

I. Introduction

GAIT rehabilitation is often focused on the legs, and overlooks the role of the upper limbs. However, studies show that there is a neural coupling between the upper and lower limbs [1], and this coupling effect can be exploited for rehabilitation of patients with walking impairment [2]–[5]. In addition, arm swing contributes to balance [6]–[8], regulates rotational body motion [9], and increases metabolic efficiency [10]. The positive effect of arm-swing integration in gait rehabilitation becomes more pronounced when patients practice correct arm-swing patterns [4]. Since it is beneficial for patients with walking impairment to combine rhythmic arm and leg movements [2], [4], [11], [12], gait rehabilitation should take the integration of arm swing into consideration.

Manuscript received March 11, 2017; revised July 10, 2017; accepted August 6, 2017. Date of publication August 15, 2017; date of current version January 8, 2018. This work was supported by the National Science Foundation under Grant 1208637. *(Corresponding author: Babak Hejrati.)*

B. Hejrati is with the Department of Mechanical Engineering, University of Maine, Orono, ME 04469 USA (e-mail: babak.hejrati@maine.edu).

A. S. Merryweather and J. J. Abbott are with the Department of Mechanical Engineering and the Robotics Center, University of Utah, Salt Lake City, UT 84112 USA (e-mail: a.merryweather@utah.edu; jake.abbott@utah.edu).

Digital Object Identifier 10.1109/TNSRE.2017.2740060

Currently, there exist several methods and technologies that attempt to include arm swing in gait rehabilitation. In one study, spinal-cord-injury patients walked on a treadmill with their arms being manually assisted by a therapist with poles [1]. In other research, sliding handrails were used for stroke patients to enable them to achieve arm swing at a faster walking speed [11]. Other studies have used recumbent stepper machines to show that active upper-limb movements increase neuromuscular activation of the lower limbs during seated recumbent stepping [13], [14]. A robotic device that involves both lower and upper limbs is presented by Yoon *et al.* [15]. In their device, the walking speed for the robot is updated based on the interactions of the robot with the user's upper limbs. In all the devices discussed thus far, upper and lower limbs are kinematically constrained with respect to one another; it is likely that what the user experiences is dissimilar to natural overground walking. More recently, our group developed a wearable robotic backpack-type device that is capable of inducing arm swing during gait rehabilitation with a body-weight-support treadmill [16].

The key open problem for the use of robotic devices that induce arm swing is how to generate proper arm-swing trajectories in real-time when patients are allowed to naturally self-select their walking speed. The generated arm-swing trajectories should be periodic (approximately sinusoidal) and have the following four key features: First, the generated trajectories should have the same fundamental frequency as the lower limbs (i.e., the stepping frequency) [2], [4], [15], [17]. Second, the generated trajectories need to maintain a correct phase relationship with lower-limb movements [17]–[20]. Third, the generated trajectories should be smooth to avoid causing discomfort for the patients when the trajectories are applied to them by a robot; in addition, applying jerky trajectories could lead to learning incorrect muscle firing patterns and an undesired gait [21]. Fourth, the amplitude of generated trajectories should change as a function of the self-selected walking speed and stepping frequency [17], [20]. In order to generate a trajectory with its frequency matching the walking frequency at any self-selected walking speed, one may consider measuring the lower-limb movement frequency in real-time, and use it to generate a sinusoidal signal for the arms. A method based on the use of a weighted Fourier linear combiner adaptive filter has been used to estimate lower trunk angle from gyroscope sensors data [22].

A band-limited multiple Fourier linear combiner has been used to estimate pathological tremor parameters from gyroscope and accelerometer sensor data [23]. Although both methods provide a means to estimate the current frequency of the input signals, both methods have been developed primarily to enable the analytical integration of inertial measurement unit (IMU) sensor data for a drift-free estimation of 3D orientation. Also, an adaptive oscillator can be used to provide an estimation of the fundamental frequency of a quasi-sinusoidal signal in real-time [24], [25]. However, if the input signals are not smooth and quasi-sinusoidal, the frequency estimation is not adequately accurate. Although the extraction of spatio-temporal gait parameters such as step frequency in real-time has been recently considered in a number of studies [26], [27], there is an inherent delay in the methods due to the detection of gait events such as heel strike. The mentioned limitations lead to either generating non-smooth signals or smooth signals with significant time lags, both of which are undesirable. Moreover, merely knowing the walking frequency is not sufficient to generate proper arm-swing trajectories because the correct phase and amplitude relationship between the generated signals and lower-limb movements has to be taken into account.

We recently conducted a study with thirty healthy adults (15 male, 15 female; body mass 49–98 kg; height 1.58–1.91 m; age 18–37 years) in which we characterized arm-swing in the sagittal plane (i.e., the amplitude, DC offset, and phase relative to contralateral heel strike of the best-fit sinusoidal trajectory) [28]. We characterized the effect of walking conditions (walking speed and surface slope) and the subjects' physical characteristics (gender, height, and weight) on arm-swing trajectory parameters, with arm swing measured at the shoulder in the sagittal plane. Although the results of this study enable us to predict the arm-swing-trajectory parameters for an average healthy adult (as well as the variance in the parameters across healthy adults) as a function of the aforementioned independent variables, the results still beg the question: How can arm-swing trajectories be generated in real-time during walking at self-selected speed?

In this paper, we propose a simple solution to generate proper arm-swing trajectories in real-time. Our fundamental conjecture is that knowledge of thigh angular velocity, measured by an IMU or motion-capture system, is sufficient to generate arm-swing trajectories in real-time that will be representative of a healthy adult's arm swing. The reason for choosing thigh angular velocities to generate arm-swing trajectories in real-time, rather than using other possible gait signals, is due to a strong correlation between arm and thigh movements during locomotion. Also, unlike hip angles, thigh angular velocities can be simply and directly measured by an IMU during walking without any additional processing. We develop a data-driven mathematical model based on the data set from [28], embodied as a linear time-invariant (LTI) transfer function, which takes a thigh's angular velocity as its input and generates a proper arm-swing trajectory as its output. With our method, we avoid the inaccuracies and complexities associated with frequency estimation in real-time, and the amplitude and phasing is handled seamlessly. We verify our method using the 30-healthy-subject data set of [28], as well as data collected from nine Parkinson patients from [29], both of which measure thigh angular velocity using optical motion tracking. We also verify that our method works with measurements taken from an IMU worn on the thigh.

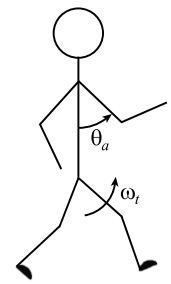

Fig. 1. A schematic representation of arm joint angle θ_a and thigh angular velocity ω_t in the sagittal plane during walking.

II. Proposed Method

We used kinematic data collected from 30 healthy subjects using an optical motion-tracking system (NaturalPoint, Corvallis, OR) during walking on a level treadmill with four equally spaced walking speeds "slow", "normal", "fast", and "fastest" with mean (standard deviation) values of 0.75 (0.26) m/s, 0.95 (0.21) m/s, 1.26 (0.22) m/s, and 1.55 (0.26) m/s, respectively [28]. The subjects were each asked to find their self-selected "normal" and "fastest" walking speeds while walking on a treadmill. Based on each subject's "normal" and "fastest" walking speeds, we calculated the midpoint between "normal" and "fastest" speeds to represent the "fast" speed; to calculate "slow" speed, we used linear extrapolation, such that "normal" speed is the midpoint between "slow" and "fast" speeds. This way, each subject tried a wide range of walking speeds based on their own natural walking speed rather than prescribed fixed speeds. The arm angle θ_a and thigh angular velocity ω_t in the sagittal plane (as illustrated in Fig. 1) were calculated as a function of time for each of the subjects' left and right arms and legs, respectively.

Our goal is to find a transfer function that takes as its input the angular velocity of the thigh $\omega_t(t)$, and generates as its output an arm-swing trajectory $\theta_a(t)$ that is consistent with what could be expected from a typical healthy adult with the same thigh angular velocity. The transfer function should capture the correct amplitude and phase relationship at the frequencies of interest for walking at self-selected speed. Furthermore, we want the transfer function to attenuate high-frequency noise in the incoming angular-velocity signal is attenuated, as well as low-frequency signals that are below the frequency at which humans walk. In this regard, we want our transfer function to behave like a band-pass filter, but with specific amplification and phasing behavior in the passband.

We utilize the first harmonic (i.e., the fundamental frequency) of the Fourier series to fit sinusoids to the thigh angular velocity of a given leg, and to the angle of the contralateral arm, as follows:

$$\omega_t = A_t \sin(ft) \tag{1}$$

$$\theta_a = A_a \sin(ft + \phi) \tag{2}$$

$$M = \frac{A_a}{A_t} \tag{3}$$

where we define T as the period of the gait cycle in seconds and $f = 2\pi/T$ as the gait frequency in rad/s. A_t and A_a are the amplitudes of thigh and arm-swing trajectories, respectively, in consistent units of either rad/s and rad, or deg/s and deg. ϕ is the phase shift in the arm angle trajectory relative to the contralateral thigh angular-velocity trajectory. M is the amplitude ratio, with units of seconds. Both M and ϕ significantly ($\alpha = 0.05$) depend on the gait frequency f with $R^2 = 9.2\%$ and $R^2 = 42.2\%$, respectively. The magnitude ratio M and phase shift ϕ, illustrated in Fig. 2 versus the gait frequency f, are used to obtain a data-driven transfer function $G(s)$ between the thighs' angular velocities and the contralateral arms' angles. Arm side (i.e., left/right) did not have a significant effect on M or ϕ, so these values for both sides are combined in Fig. 2.

Although subjects' height was found to be a significant independent variable for both M and ϕ, it only accounted for small portions of variances ($R^2 = 5.9\%$ for M and $R^2 = 1.7\%$ for ϕ). Also, the DC offset values of the arms' angle trajectories (defined from a neutral position) were found to significantly dependent on subjects' height; however, the effect size of height was found to be small ($R^2 = 2.3\%$). The mean value (with 95% confidence interval) of the arm-trajectories' DC offset values were found to be $0.47°(0.13°, 0.81°)$; since the mean value is small, we neglected the offset value for generating the arm-swing trajectory (we subsequently neglected to include an offset term in (2)). By neglecting the small effect of height, and by neglecting the offset in the arm-swing trajectory, we are able to obtain the simple "one size fits all" LTI transfer function $G(s)$ that is not unnecessarily complicated.

Our initial candidate transfer function had a zero at $s = 0$ to filter DC signals and two poles to filter high-frequency noise. We found that to perform proper filtering of noisy thigh angular-velocity sensors, our transfer function required a sharp roll-off at frequencies only slightly above the maximum walking frequencies. We used the MATLAB (Mathworks, Natick, MA) System Identification Toolbox to increase the number of poles until we achieved the desired specifications while simultaneously creating a frequency response similar to that of experimental data in the walking frequency range. We prioritized achieving the full set of design specifications over achieving a "best fit" of the data. The following transfer function represents our final data-driven model:

$$G(s) = \frac{1200s}{s^5 + 58s^4 + 280s^3 + 3900s^2 + 7700s + 730} \tag{4}$$

To implement the transfer function in real-time software, we used MATLAB to convert $G(s)$ to a discrete state-space form using the Tustin discretization method.

The arm-swing trajectory for a given arm can be directly generated using the contralateral thigh's angular velocity ω_{tc}:

$$\theta_a(s) = G(s)\omega_{tc}(s) \tag{5}$$

Since the phase difference between the two arms is 180° (since we neglect any DC offset term), the trajectory for the other arm can be generated simply by using the negative of the trajectory

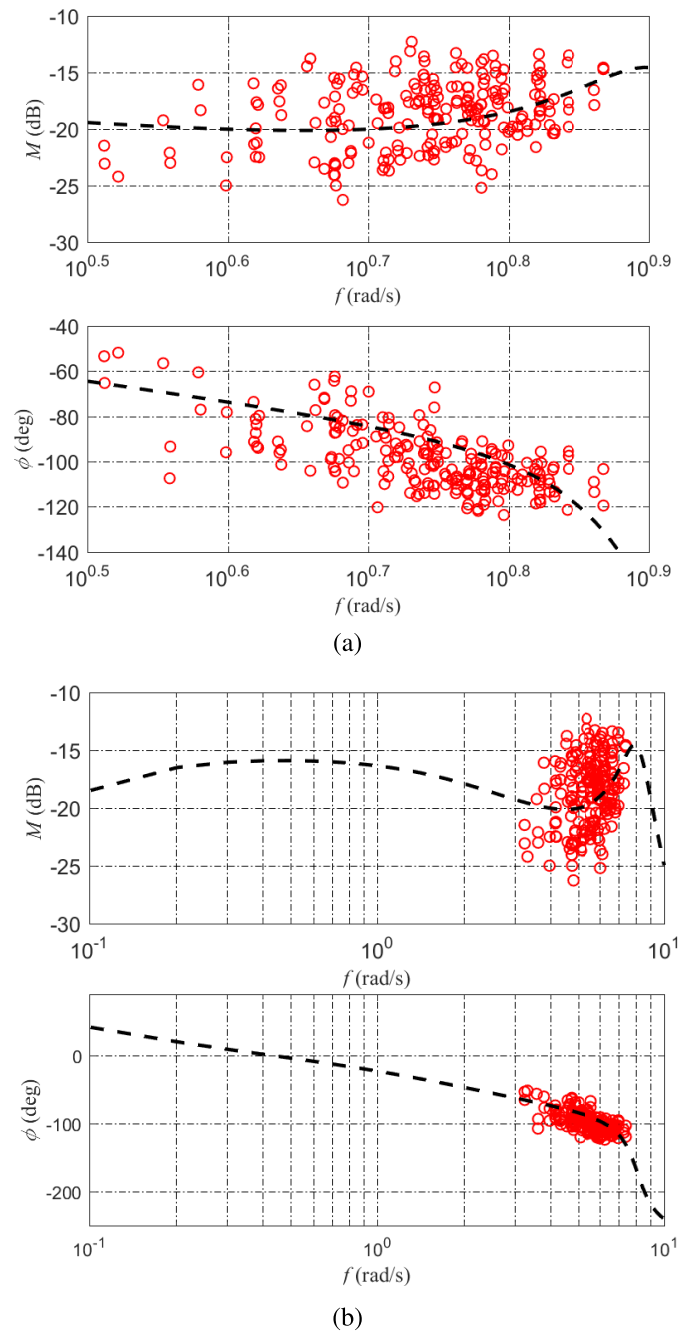

Fig. 2. Bode diagram of $G(s)$ (black dashed line) within the walking frequency range (a), and over a wider range (b), in which red circles represent experimental amplitude ratios M and phase shifts ϕ between arms' angles and their corresponding contralateral thighs' angular velocities.

already generated; this method would only require the angular velocity of a single thigh to generate arm-swing trajectories for both arms. Alternatively, the trajectory for a given arm can be generated as the average of trajectories generated by each of the contralateral and ipsilateral thighs' angular velocities:

$$\theta_a(s) = G(s)\left(\frac{\omega_{tc}(s) - \omega_{ti}(s)}{2}\right) \tag{6}$$

We will show that this averaging method is more robust to pathological gait, and is the method that should be used.

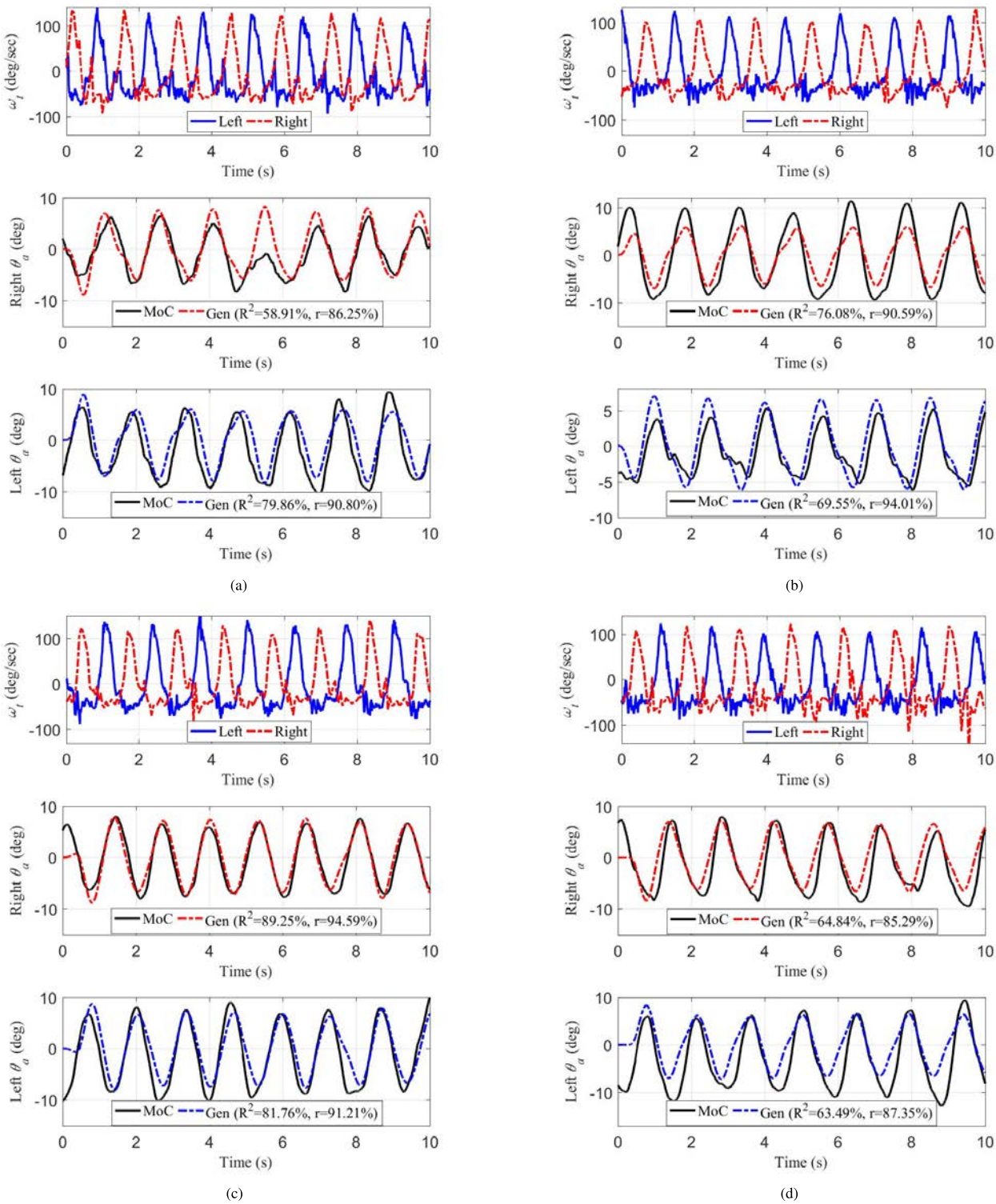

Fig. 3. Left and right thigh angular velocities from motion-capture, the resulting generated arm-swing trajectories (using (6)), and actual arm-swing trajectories (from motion-capture), of four healthy subjects walking with their "slow" self-selected speeds. These speeds closely match the walking speed of individuals with pathological gait. The motion-capture trajectories correspond to steady-state walking, whereas the generated arm-swing trajectories are initialized at zero to demonstrate a transient response. (a) Subject A walking at 0.52 m/s. (b) Subject B walking at 0.44 m/s. (c) Subject C walking at 0.57 m/s. (d) Subject D walking at 0.66 m/s.

III. Experimental Validation

To evaluate the performance of the proposed method with respect to the four criteria described in Section I, we apply the method in (6) to the thigh angular velocities from the complete data set in [28] to generate arm-swing trajectories. As demonstrated in Fig. 3, the generated trajectories have strong correlations with the motion-capture reference trajectories. Due to the use of an LTI model, there is a perfect agreement between

TABLE I
COEFFICIENTS OF DETERMINATION R^2, AND CORRELATION COEFFICIENTS r, BETWEEN GENERATED AND MOTION-CAPTURE TRAJECTORIES, WITH VALUES REPORTED AS MEAN (95% CONFIDENCE INTERVAL) OVER $N = 108$ TRIALS

Parameter	Left	Right	p-value
R^2	0.68 (0.64,0.72)	0.66 (0.62,0.70)	$p = 0.43$
r	0.91 (0.89,0.92)	0.90 (0.89,0.92)	$p = 0.82$

the frequencies of generated and actual arm-swing trajectories. We used the coefficient of determination R^2 and correlation coefficient r as metrics to assess the similarity between the arm-swing trajectories generated using our method and the actual trajectories observed with the motion-capture system. The coefficient of determination R^2 and correlation coefficient r between the generated and motion-capture trajectories for the left arm and right arm are presented in Table I with $N = 108$ per arm. The values of R^2 and r for the left arms' trajectories were not statistically different from those for the right arms' trajectories. If any difference does exist between arms, its effect size would be small. In subsequent analysis, we combine the left- and right-arm data to effectively double the number of trials to $N = 216$.

Despite the non-smooth nature of the thigh angular velocities, the generated trajectories are adequately smooth. Flash and Hogan [30] found that, when humans conduct point-to-point movements, they tend to adopt minimum-jerk trajectories that can be well described by fifth-order polynomials. Thus, we divided each generated trajectory within a gait cycle in two parts (i.e., the forward-swing phase and the backward-swing phase) to compare each part with a best-fit fifth-order polynomial function between two target points (i.e., maximum and minimum points). The mean value ($\pm$ standard deviation) of R^2 between the generated trajectories and their fifth-order fits is 99.50% ($\pm$0.87%) indicating a high degree of smoothness in the generated trajectories.

We utilized point relative phase (PRP) and amplitude difference [11], [28], both in degrees, between the actual and generated trajectories in gait cycle (j) to represent the model's phase (E_{phase}) and amplitude (E_{amp}) errors, respectively:

$$E_{phase}(j) = \frac{t_{max,Gen}(j) - t_{max,MoC}(j)}{t_{cycle}(j)} \times 360^\circ \quad (7)$$

$$Amp = \frac{Max(j) - Min(j)}{2} \quad (8)$$

$$E_{amp}(j) = Amp_{MoC} - Amp_{Gen} \quad (9)$$

where gait cycle j was determined by two consecutive local peaks of the shoulder angle, $t_{cycle}(j)$ represents the time duration of cycle j, $t_{max,Gen}(j)$ is the time of generated trajectory's peak in cycle j, and $t_{max,MoC}(j)$ is the time of shoulder angle trajectory's peak in the motion-capture data. In (8), Amp is the amplitude of a trajectory in gait cycle j, which is defined based on the maximum $Max(j)$ and minimum $Min(j)$ of the trajectory within gait cycle j. Table II shows the mean value of E_{phase} and E_{amp} for the complete data set of $N = 216$ trials (with each trial comprising approximately 6–10 gait cycles of a given subject at a given steady-state speed).

TABLE II
WITHIN-TRIAL MEAN ERROR IN THE AMPLITUDE AND PHASE OF THE GENERATED TRAJECTORY RELATIVE TO THE MEASURED TRAJECTORY, AND WITHIN-TRIAL STANDARD DEVIATION IN THE AMPLITUDE AND PHASE OF THE MEASURED TRAJECTORY, WITH VALUES REPORTED AS MEAN ($\pm$ STANDARD DEVIATION) OF THOSE QUANTITIES OVER $N = 216$ TRIALS

Parameter	Mean error in generated values	Standard deviation in measured values
Amplitude	$1.12^\circ(\pm 4.45^\circ)$	$2.18^\circ(\pm 1.08^\circ)$
Phase	$1.57^\circ(\pm 10.85^\circ)$	$7.61^\circ(\pm 3.70^\circ)$

When a healthy person walks, there is substantial variation in the parameters of their arm swing, even when walking at a constant speed. This type of variation is not observed in our generated trajectories, which are much more deterministic. As a result, there will typically be some amount of error when comparing the generated trajectory to the actual trajectory of any healthy subject. To quantify intrasubject phase and amplitude variations, we used the standard deviation of PRP between shoulder angles and their contralateral thigh angular velocities $PRP_{sh/th}$ (defined analogously to (7)) and the standard deviation of shoulder-angle amplitudes Amp_{sh} across multiple gait cycles within a given trial. The standard deviations of $PRP_{sh/th}$ and Amp_{sh} quantify how a given subject changes their arm-swing trajectory across various gait cycles during steady-state walking at a specific speed. We can compute the mean and standard deviation (across $N = 216$ individual trials) in these standard deviations, which enables us to quantify the types a variation that occurs in arm swing in the population of healthy adults. Table II indicates that our model's errors are reasonable when we consider the variance observed in the population of healthy adults and are within reasonable ranges of within-trial variations.

IMUs are commonly used to measure angular velocities of human body segments in real-time. Since IMUs have different noise properties than motion-capture systems, we tested our proposed method using thigh angular velocities measured by an IMU. We conducted an experiment with six healthy adult subjects, with the approval of the Institutional Review Board of the University of Utah. The subjects wore an IMU (a triple axis accelerometer and gyroscope, MPU-6050) either on their left or right thigh (three subjects each) during walking. Since each subject only used one IMU, we generated an arm-swing trajectory for the contralateral arm by applying (5), and then applied the negative trajectory to the ipsilateral arm. Figure 4 demonstrates four examples of arm-swing trajectories in which thigh angular velocity was measured by an IMU. The generated trajectories again have strong correlations with the motion-capture reference trajectories.

Although we can observe the transient response of our LTI transfer function $G(s)$ in Figs. 3 and 4 (because the output is initialized at zero), in those experiments, the subject is already walking at a steady-state speed at the beginning of data collection. We want to ensure that our method works equally well when the subject changes walking speed during locomotion. Figure 5 shows a typical generated trajectory when a

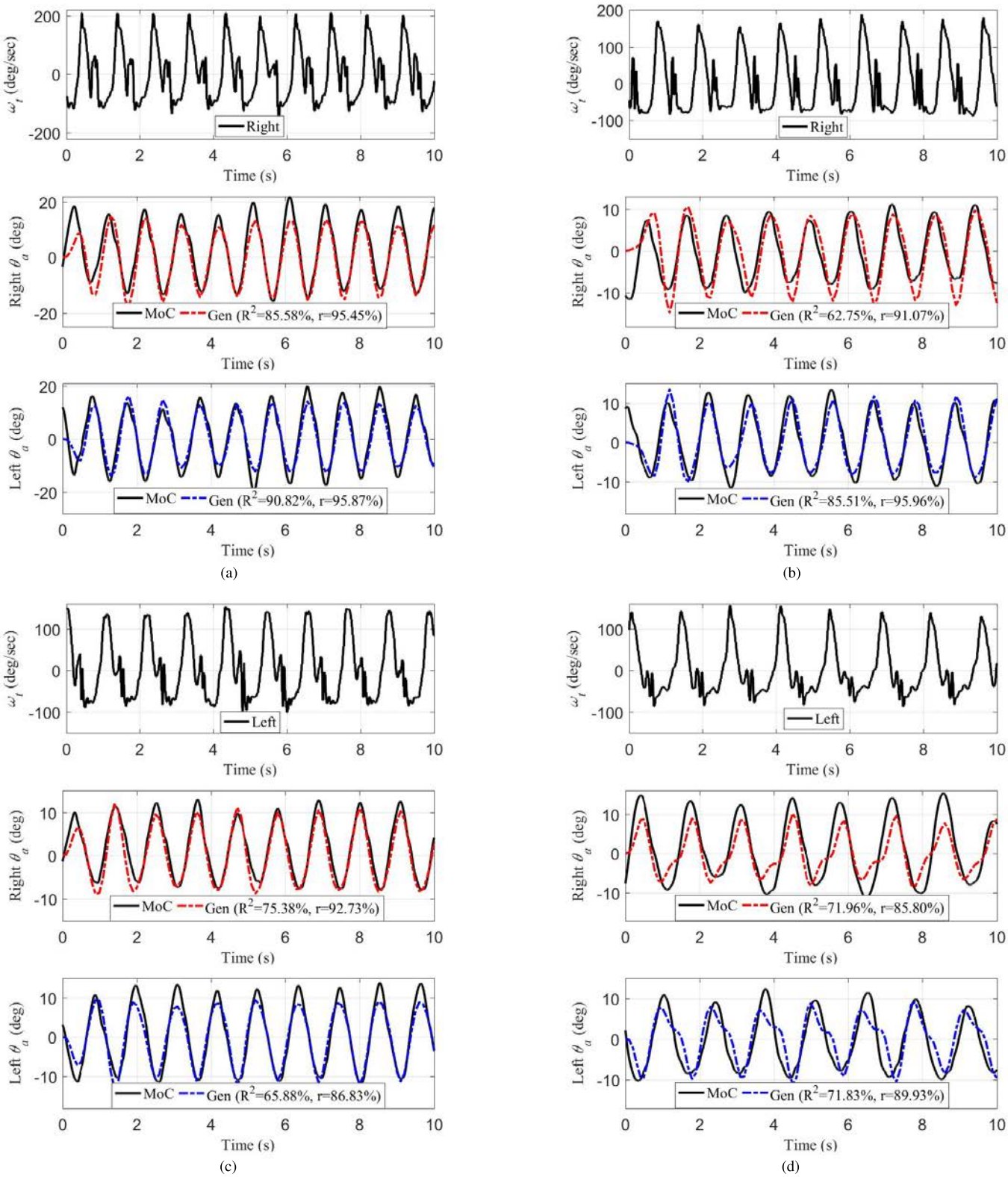

Fig. 4. Left or right thigh angular velocity from IMU, the resulting generated arm-swing trajectories (using (5)), and actual arm-swing trajectories (from motion-capture), of four typical healthy subjects with a spread of self-selected walking speeds. The motion-capture trajectories correspond to steady-state walking, whereas the generated arm-swing trajectories are initialized at zero to demonstrate a transient response. (a) Subject E walking at 1.4 m/s. (b) Subject F walking at 1.1 m/s. (c) Subject G walking at 1.2 m/s. (d) Subject H walking at 0.6 m/s.

subject starts walking from rest and then reaches a steady-state walking speed. The generated trajectory starts at 0° during the standing phase, and it increases in a well-behaved pattern as the contralateral thigh's angular velocity increases while the subject approaches a steady-state walking speed. Since the trajectory is generated in response to the thigh angular

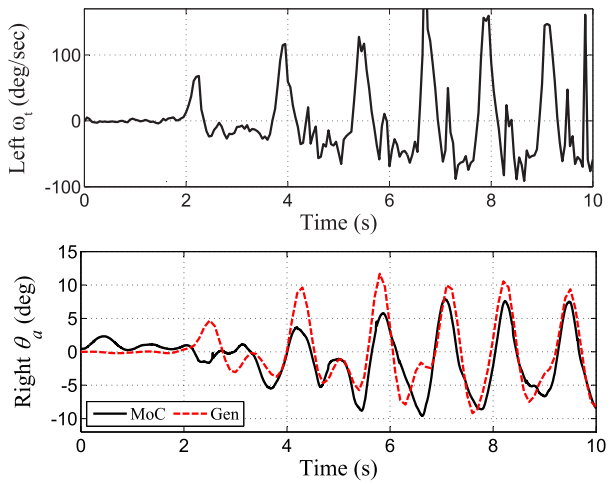

Fig. 5. Generating an arm-swing trajectory (using IMU data) while a subject transitions from standing to walking.

TABLE III
DEMOGRAPHICS OF PARKINSON PATIENTS FROM [29] WITH VALUES REPORTED AS MEAN (± STANDARD DEVIATION)

Female	3
Male	6
Age	67.67 (±7.05)
Mass (kg)	80.98 (±20.58)
Height (m)	1.66 (±0.16)
UPDRS score	36.13 (±11.78)
H&Y score	2.39 (±0.31)

velocity, we observe in Fig. 5 that it anticipates arm swing a full cycle before it is actually observed in the motion-capture data. Figure 6 shows another typical generated trajectory in which a subject increases and then decreases walking speed and stepping frequency during walking. As the zoomed plots in Fig. 6 illustrate, the generated trajectory quickly adapts to the changes in the thigh angular velocity and maintains proper frequency and phase behaviors compared to the actual arm-swing trajectory.

Up to this point, only thigh movements of *healthy* subjects have been considered for generating arm-swing trajectories (both in terms of creating our data-driven model, and in terms of validating the model). However, it is important to evaluate our proposed method when applied to patients with pathological gait, whose thigh movements are themselves pathological. We applied the method in (6) to the gait data of nine Parkinson patients collected by Merryweather *et al.* [29]. Table III shows the demographics for the patients, in which patients' physical characteristics, unified Parkinson disease rating scale (UPDRS), and Hoehn and Yahr scale (H&Y) are presented. Figure 7 shows the generated trajectories for the right and left arms of the patients given their thigh angular velocity, obtained from motion-capture. The proposed method could successfully generate smooth trajectories (i.e., with R^2 of 99.06% (±1.15%) of the best-fit fifth-order polynomials) for the patients at their self-selected walking speeds. To demonstrate how the proposed method may be beneficial for the patients, we compared their arm-swing patterns with the range of arm-swing patterns that could be expected from healthy people walking at the same stepping frequency.

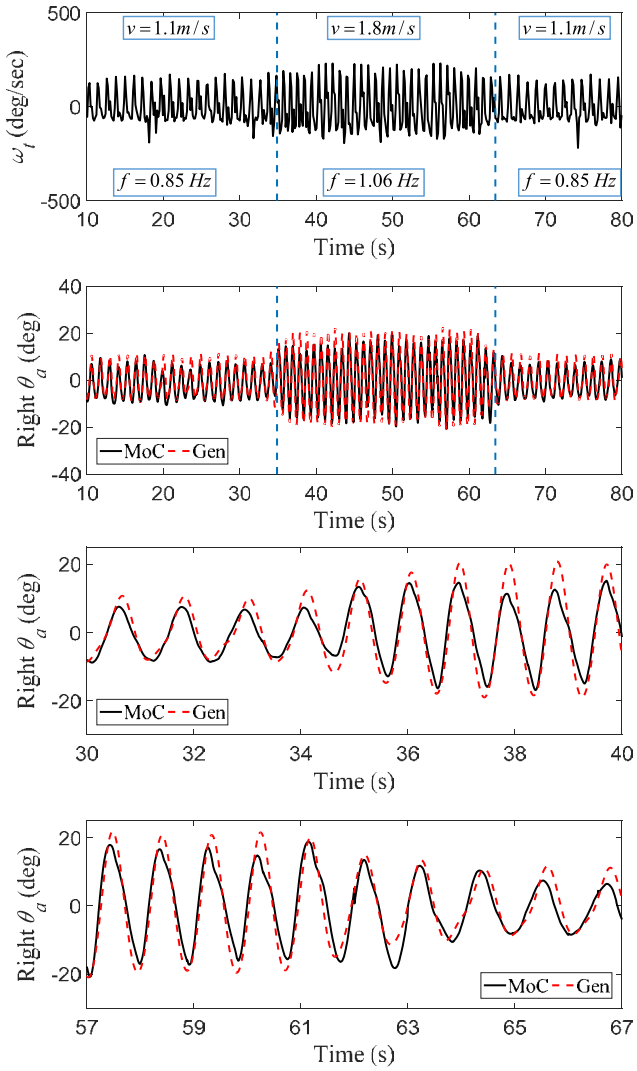

Fig. 6. Generating an arm-swing trajectory (using IMU data) while a subject increases and then decreases walking speed.

First, we evaluated the prediction bounds with 95% confidence [31] for the phase and magnitude data in Fig. 2. The prediction bounds define the lower and upper values of the interval that the new observations will fall into with 95% likelihood. Then, we used each patient's walking frequency and thigh angular velocity to specify a range of normal arm-swing patterns for the patient. Figure 7 shows the patients' arm-swing patterns along with the generated ones and normal ranges. Clearly, most of the patients do not demonstrate proper arm swing. Absence of arm swing, asymmetry of motion, irregular patterns, and improper relative phase can be observed in the patients' data, which may highlight the necessity of arm-swing assistance for these patients. Not only does the generated trajectory for each patient fall into the normal range, but also it looks more proper than the patient's actual arm swing.

We found that using only one thigh's angular velocity using (5) to generate arm-swing trajectories works satisfactorily for many cases, including most healthy subjects and some pathological subjects. However, Fig. 8 shows an example where the generated arm-swing trajectory for a Parkinson patient using only one thigh was substantially less smooth than the trajectory generated by measuring both thighs and

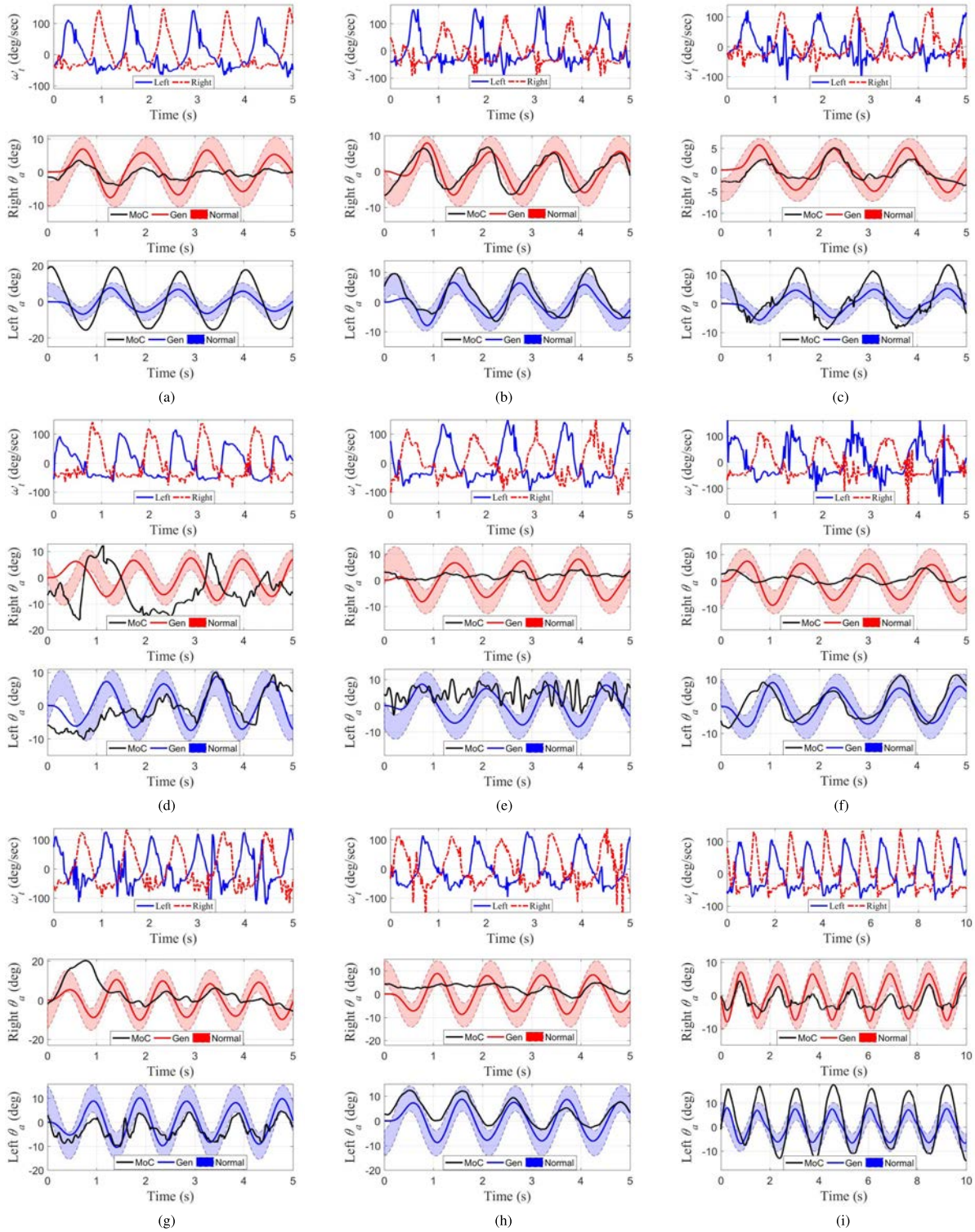

Fig. 7. Left and right thigh angular velocities and actual arm-swing trajectories from motion-capture, the resulting generated arm-swing trajectories (using (6)), and normal arm-swing ranges for nine Parkinson patients. (a) Patient A walking at 0.57 m/s. (b) Patient B walking at 0.60 m/s. (c) Patient C walking at 0.58 m/s. (d) Patient D walking at 0.57 m/s. (e) Patient E walking at 0.57 m/s. (f) Patient F walking at 0.50 m/s. (g) Patient G walking at 0.58 m/s. (h) Patient H walking at 0.51 m/s. (i) Patient I walking at 0.54 m/s.

using (6). We observed a similar response in the healthy-subject trial shown in Fig. 4(d). We conclude that measuring both thighs' angular velocities and using (6) is the recommended method for use.

IV. Discussion

The results of this study show that the generated arm-swing trajectories satisfied our desired criteria. By using a data-driven LTI transfer function, the generated arm-swing trajectories

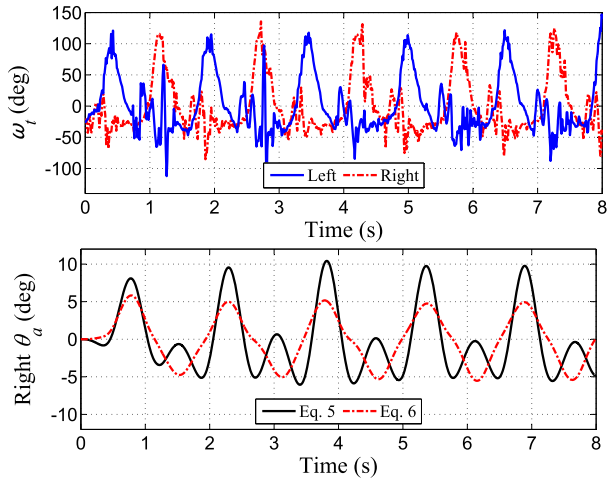

Fig. 8. Left and right thigh angular velocities of a Parkinson patient, right arm-swing trajectories generated by (5) using only the left thigh angular velocity, and generated by (6) using both left and right thigh angular velocities.

inherently have the same frequency as the lower limbs at any self-selected speed, which is essential for coordinated walking. The proposed method generates trajectories that have proper phase relationships with respect to the gait cycle throughout the full range of walking frequencies. Despite the non-smooth nature of thigh angular velocities, our transfer function's inherent filtering of high-frequency noise, combined with the averaging implemented in (6), results in smooth signals that could be applied to patients' arms during gait rehabilitation by robotic or other rehabilitation devices without causing discomfort. It should be noted that our method is not intended to be predictive of arm swing in any given healthy individual, rather, it is intended to generate a reasonable arm-swing trajectory for a patient for which there will be no healthy baseline for comparison. The quantitative validation of our method, described in Tables I and II, should be interpreted with this in mind.

The application of the proposed method is in devices that attempt to integrate arm swing in gait rehabilitation [16]. Because our "one size fits all" transfer function was created based on 30 healthy subjects who exhibited a substantial amount of intersubject variation, it would be incorrect to assume that a patient must rigidly follow the generated trajectory for their arm swing to be considered healthy. More effective patient-cooperative approaches allow deviation from predefined reference trajectories. An impedance-control approach can be considered as a less strict method in which the generated reference trajectory is coupled with the patient's actual shoulder angle through a virtual compliance to individualize rehabilitation by adjusting these parameters [32]. A "path control" strategy and other related approaches provide a virtual tunnel around the reference trajectory in which patients can move their limbs with their own timing and amplitude of movements [33]. These methods enable patient-cooperative robot-aided gait rehabilitation and increase patients' active participation in gait rehabilitation.

It may also be possible to use the generated trajectory as a baseline reference signal upon which other types of rehabilitation approaches can be explored. For example, the magnitude of the generated trajectory can be altered by simply multiplying the LTI transfer function by a constant or adaptive gain to create deliberate changes in arm-swing amplitude [34]. Alternatively, the generated trajectories can be utilized to generate continuous or discrete tactile feedback to enhance arm-leg coupling [35].

Given that various walking impairments may result in different pathological gait patterns, one single method may not be sufficient to generate arm-swing trajectories for patients with different walking impairments. Future work should apply our method to a variety of gait pathologies, such as spinal cord injury and stroke, and use a larger sample size to determine which pathological gaits can be addressed by our proposed method directly. In addition, future research may consider the relationship between arm-swing trajectories and the motion of other body segments, such as torso rotation or heel-strike, during walking with self-selected speed. It may be possible to apply the techniques used in this paper to generate a new LTI transfer function whose input is one of the aforementioned signals, and this new transfer function may be as good (or even better) at generating of proper arm swing for patients. However, it should be noted that it may be that the method proposed in this paper can be applied, without modification, to a variety of gait pathologies.

V. Conclusions

We proposed a method for generating proper arm-swing trajectories in real-time using only measurements of the angular velocity of a person's thighs, to be used during gait rehabilitation with self-selected walking speed. A data-driven linear time-invariant transfer function was developed, using frequency-response methods, which captures the frequency-dependent magnitude and phase relationship between the thigh angular velocities and the arm angles (measured at the shoulder, in the sagittal plane), using a data set of 30 healthy adult subjects. The proposed method generates smooth trajectories that have high correlations with the actual measured trajectories of the healthy individuals. The method was verified on gait data gathered from patients with Parkinson disease, and even their pathological thigh trajectories resulted in proper arm-swing trajectories. The proposed method can be used in future robotic devices that integrate arm swing in gait rehabilitation.

Acknowledgment

The authors would like to thank Dr. Kam K. Leang for his valuable advice regarding frequency-response methods.

References

[1] A. L. Behrman and S. J. Harkema, "Locomotor training after human spinal cord injury: A series of case studies," *Phys. Therapy*, vol. 80, no. 7, pp. 688–700, 2000.

[2] D. P. Ferris, H. J. Huang, and P. C. Kao, "Moving the arms to activate the legs," *Exerc. Sport Sci. Rev.*, vol. 34, no. 3, pp. 113–120, 2006.

[3] D. S. Marigold and J. E. Misiaszek, "Whole-body responses: Neural control and implications for rehabilitation and fall prevention," *Neuroscientist*, vol. 15, no. 1, pp. 36–46, Feb. 2009.

[4] D. de Kam, J. Duysens, and V. Dietz, "Do we need allowing arm movements for rehabilitation of gait?" in *Converging Clinical and Engineering Research on Neurorehabilitation* (Biosystems & Biorobotics). Berlin, Germany: Springer-Verlag, 2013, pp. 959–962, doi: https://doi.org/10.1007/978-3-642-34546-3_156

[5] J. L. Stephenson, S. J. De Serres, and A. Lamontagne, "The effect of arm movements on the lower limb during gait after a stroke," *Gait Posture*, vol. 31, pp. 109–115, Jan. 2010.

[6] S. M. Bruijn, O. G. Meijer, P. J. Beek, and J. H. van Dieën, "The effects of arm swing on human gait stability," *J. Experim. Biol.*, vol. 213, no. 23, pp. 3945–3952, 2010.

[7] M. Punt, S. M. Bruijn, H. Wittink, and J. H. van Dieën, "Effect of arm swing strategy on local dynamic stability of human gait," *Gait Posture*, vol. 41, pp. 504–509, Feb. 2015.

[8] Y. Wu *et al.*, "Effect of active arm swing to local dynamic stability during walking," *Human Movement Sci.*, vol. 45, pp. 102–109, Feb. 2016.

[9] H. Elftman, "The function of the arms in walking," *Human Biol.*, vol. 11, no. 4, pp. 529–535, 1939.

[10] S. H. Collins, P. G. Adamczyk, and A. D. Kuo, "Dynamic arm swinging in human walking," *Proc. R. Soc. Lond. B, Biol. Sci.*, vol. 276, no. 1673, pp. 3679–3688, 2009.

[11] J. L. Stephenson, A. Lamontagne, and S. J. De Serres, "The coordination of upper and lower limb movements during gait in healthy and stroke individuals," *Gait Posture*, vol. 29, no. 1, pp. 11–16, 2009.

[12] F. Sylos-Labini, Y. P. Ivanenko, M. J. MacLellan, G. Cappellini, R. E. Poppele, and F. Lacquaniti, "Locomotor-like leg movements evoked by rhythmic arm movements in humans," *PLoS ONE*, vol. 9, no. 3, p. e90775, 2014.

[13] P.-C. Kao and D. P. Ferris, "The effect of movement frequency on interlimb coupling during recumbent stepping," *Motor Control*, vol. 9, no. 2, pp. 144–163, 2005.

[14] H. J. Huang and D. P. Ferris, "Neural coupling between upper and lower limbs during recumbent stepping," *J. Appl. Physiol.*, vol. 97, no. 4, pp. 1299–1308, 2004.

[15] J. Yoon, B. Novandy, C.-H. Yoon, and K.-J. Park, "A 6-DOF gait rehabilitation robot with upper and lower limb connections that allows walking velocity updates on various terrains," *IEEE/ASME Trans. Mechatronics*, vol. 15, no. 2, pp. 201–215, Apr. 2010.

[16] O. R. Barnes, B. Hejrati, and J. J. Abbott, "An underactuated wearable arm-swing rehabilitator for gait training," in *Proc. IEEE Int. Conf. Robot. Autom.*, May 2015, pp. 4998–5003.

[17] M. P. Ford, R. C. Wagenaar, and K. M. Newell, "Arm constraint and walking in healthy adults," *Gait Posture*, vol. 26, no. 1, pp. 135–141, 2007.

[18] J. Yoon, J. Park, and J. Ryu, "A planar symmetric walking cancellation algorithm for a foot–platform locomotion interface," *Int. J. Robot. Res.*, vol. 29, no. 1, pp. 39–59, 2010.

[19] M. Kubo, R. C. Wagenaar, E. Saltzman, and K. G. Holt, "Biomechanical mechanism for transitions in phase and frequency of arm and leg swing during walking," *Biol. Cybern.*, vol. 91, no. 2, pp. 91–98, 2004.

[20] H. Carpinella, P. Crenna, M. Rabuffetti, and M. Ferrarin, "Coordination between upper- and lower-limb movements is different during overground and treadmill walking," *Eur. J. Appl. Physiol.*, vol. 108, no. 1, pp. 71–82, 2010.

[21] N. J. Tester, D. R. Howland, K. V. Day, S. P. Suter, A. M. Cantrell, and A. L. Behrman, "Device use, locomotor training and the presence of arm swing during treadmill walking after spinal cord injury," *Spinal Cord*, vol. 11, no. 49, pp. 451–456, 2011.

[22] V. Bonnet, C. Mazzà, J. McCamley, and A. Cappozzo, "Use of weighted Fourier linear combiner filters to estimate lower trunk 3D orientation from gyroscope sensors data," *J. Neuroeng. Rehabil.*, vol. 10, p. 29, Mar. 2013.

[23] K. C. Veluvolu and W. T. Ang, "Estimation of physiological tremor from accelerometers for real-time applications," *Sensors*, vol. 11, no. 3, pp. 3020–3036, 2011.

[24] R. Ronsse, N. Vitiello, T. Lenzi, J. van den Kieboom, M. C. Carrozza, and A. J. Ijspeert, "Human–robot synchrony: Flexible assistance using adaptive oscillators," *IEEE Trans. Biomed. Eng.*, vol. 58, no. 4, pp. 1001–1012, Apr. 2011.

[25] R. Ronsse *et al.*, "Oscillator-based assistance of cyclical movements: Model-based and model-free approaches," *Med. Biol. Eng. Comput.*, vol. 49, pp. 1173–1185, Oct. 2011.

[26] S. R. Hundza *et al.*, "Accurate and reliable gait cycle detection in Parkinson's disease," *IEEE Trans. Neural Syst. Rehabil. Eng.*, vol. 22, no. 1, pp. 127–137, Jan. 2014.

[27] A. Ferrari, P. Ginis, M. Hardegger, F. Casamassima, L. Rocchi, and L. Chiari, "A mobile Kalman-filter based solution for the real-time estimation of spatio-temporal gait parameters," *IEEE Trans. Neural Syst. Rehabil. Eng.*, vol. 24, no. 7, pp. 764–773, Jul. 2016.

[28] B. Hejrati, S. Chesebrough, K. B. Foreman, J. J. Abbott, and A. S. Merryweather, "Comprehensive quantitative investigation of arm swing during walking at various speed and surface slope conditions," *Human Movement Sci.*, vol. 49, pp. 104–115, Oct. 2016.

[29] A. Merryweather, M. Hunt, L. Smith, B. Foreman, and M. Minor, "Gait alterations on irregular terrain in older adults with and without Parkinson disease: Fall risk implications," in *Proc. 19th Triennial Congr. IEA*, 2015, p. 14.

[30] T. Flash and N. Hogan, "The coordination of arm movements: An experimentally confirmed mathematical model," *J. Neurosci.*, vol. 5, no. 7, pp. 1688–1703, Jul. 1985.

[31] M. W. Lenhoff, T. J. Santner, J. C. Otis, M. G. E. Peterson, B. J. Williams, and S. I. Backus, "Bootstrap prediction and confidence bands: A superior statistical method for analysis of gait data," *Gait Posture*, vol. 9, pp. 10–17, Mar. 1999.

[32] A. Duschau-Wicke, A. Caprez, and R. Riener, "Patient-cooperative control increases active participation of individuals with SCI during robot-aided gait training," *J. Neuroeng. Rehabil.*, vol. 7, p. 43, Sep. 2010.

[33] A. Duschau-Wicke, J. von Zitzewitz, A. Caprez, L. Lünenburger, and R. Riener, "Path control: A method for patient-cooperative robot-aided gait rehabilitation," *IEEE Trans. Neural Syst. Rehabil. Eng.*, vol. 18, no. 1, pp. 38–48, Feb. 2010.

[34] S. T. Eke-Okoro, M. Gregoric, and L. E. Larsson, "Alterations in gait resulting from deliberate changes of arm-swing amplitude and phase," *Clin. Biomech.*, vol. 12, pp. 516–521, Oct./Nov. 1997.

[35] E. P. Zehr *et al.*, "Enhancement of arm and leg locomotor coupling with augmented cutaneous feedback from the hand," *J. Neurophysiol.*, vol. 98, no. 3, pp. 1810–1814, 2011.